10th International Workshop on Research and Education in Mechatronics
September 10th-11th 2009, Glasgow, UK

CONTROL SYSTEM DEVELOPMENT FOR A DEXTEROUS ROBOT HAND WITH REMOTELY LOCATED ACTUATORS AND SENSORS

David J. Cassar, Michael A. Saliba*

University of Malta, Department of Industrial and Manufacturing Engineering, Msida, Malta MSD 2080

Abstract: In this work we report on the improvements to the actuation system, as well as on the detailed position and force sensor calibration, for an anthropomorphic robot hand with remotely located actuators and sensors. The preliminary development of a computer-based control system is also described. We show that the concept of sensing the force and position of the robot fingers remotely, through actuating cable tension and position measurement, is achievable for teleoperator applications.

Key words: anthropomorphic, robot hands, tendon technology, teleoperation

I INTRODUCTION

The UOM Robot Hand, introduced in [1], is an anthropomorphic gripper. This means that it is an end effector which is similar in appearance and function to the human hand, with human biology used as the source of inspiration in its creation. Anthropomorphic hands have the outstanding advantage of versatility with regards to the grasping of objects of different shapes and sizes. In order to attain this goal, it is beneficial to have a dexterous robot hand with a sufficient number of degrees of freedom, as well as a sensing system of the highest quality. However, the number of actuators and sensors required, if placed on the hand itself, would in general increase the weight of the hand, thus reducing its payload. They may also interfere with the grasping of objects. An approach which avoids this problem is to place the actuators and sensors remotely located from the hand.

Remote actuation can be achieved through a cable transmission system; a mechanism similar to the way human muscles function. The latter consist of small muscles located in the human hand. However, the movement of the hand is mainly attributed to flexor and extensor muscles located in the forearm [2]. An imitation of this biological system has been successfully developed in a number of well known anthropomorphic robotic hands, such as the Utah/Mit Hand, developed in 1983 [3], the UB Hand II (1992) [4], and the DIST-Hand (1998) [5]. As can be seen, the concept of remote actuation has been included even in some of the first anthropomorphic hands. This is because, early in the development of this research area, it was understood that the reduction of the weight of the hand is crucial, and that this weight reduction could potentially be achieved through remote actuation.

Unlike actuation, remote sensing is uncommon in robotic hands. One may argue that remote sensing is not a necessity since the increase in weight using sensors currently available is very minimal. Although this may be true for some sensors, there are other disadvantages when using on-board sensors. When attached to the hand, sensors may constrain certain movements and grasping that the particular anthropomorphic robotic hand might have otherwise been able to perform. This is most critical for the fingertips of the robotic hand. One must also keep in mind that certain sensors may not withstand some of the conditions to which the robotic hand might be exposed, such as extreme temperatures and pressures as well as vibrations and impacts. Through remote sensing, the particular sensors used may be placed in a safe remote location.

II BASIC DESIGN OF THE UOM ROBOT HAND

With the growth of interest towards humanoid robots, anthropomorphism of robotic hands became a necessary design goal [6]. The UOM Robot Hand, a project which commenced in late 2005, was preceded by a number of projects in the same lab, the Industrial Automation Laboratory (IAL) of the Department of Industrial and Manufacturing Engineering (DIME) at the University of Malta. These projects provided important results, and were the preliminary steps in the path towards building an anthropomorphic robot hand in the lab. Amongst these projects are a three-fingered, nine-joint gripper [7], a five degree-of-freedom (DOF) hand and wrist system [8], as well as a three DOF anthropomorphic robot finger [9]. Other relevant projects include a biologically inspired gripper slip sensor [10] and a detailed dexterity study [11]. These projects provided a number of guidelines

* *corresponding author, email: michael.saliba@um.edu.mt*

which helped in the design of the UOM robot hand described briefly in the following paragraph.

The UOM Robot Hand is described in detail in [1]. It has three fingers and a thumb. The fingers are made of stainless steel links, with aluminium pulleys at each joint. The joints are located at positions similar to ones found in the human hand. Each finger has three flexion joints with two degrees of freedom, at the inner, or MCP, joint, and the middle, or PIP, joint. The outermost, or DIP, joint, is coupled to the PIP joint. With this coupling, when the PIP joint is driven through an angle θ, the DIP joint is made to rotate by an angle of ⅔θ. It works for both flexion and extension of the joint without the need for a return spring. The human fingers are however equipped with yet another DOF. This occurs at the carpometacarpal (CMC) joint, located at the base of the metacarpal bone of each finger. While this joint allows the human fingers very limited motion which could be omitted in the robot hand design, it allows the human thumb another vital DOF. As a result, the thumb of the developed robotic hand has a rotary degree of freedom and two coupled flexion joints. The eight DOF hand designed is shown in Figure 1. From the photo presented, one can clearly understand that the robotic hand created is very similar in appearance to the human hand. It is also similar in function; however one must understand that it is very difficult to replicate the human hand: a twenty-one DOF organ which has developed over millions of years.

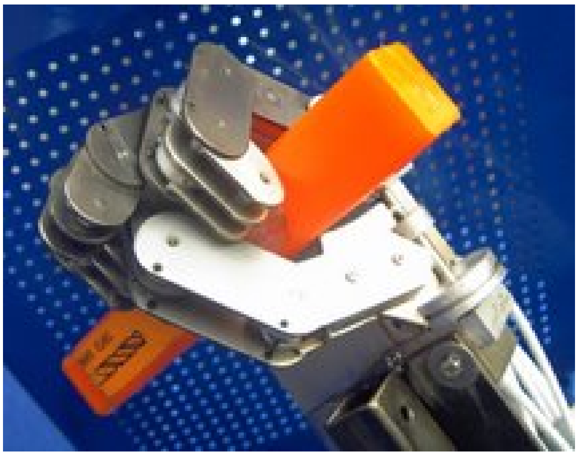

Figure 1: The UOM Robot Hand (reproduced from [1])

The actuation system of the hand is made up of eight DC motors, one for every DOF. Each motor is linked to a reduction gearbox and a leadscrew, and connected to one finger joint through a cable transmission system. This cable transmission system is analogous to the tendon system found in the human hand. Before the upgrading of the UOM Robot Hand took place, the basic design was based on single acting actuation systems. Finger joints opened through a return spring mechanism.

The UOM Robot Hand is also equipped with the position and force sensors illustrated in Figure 2 and Figure 3 respectively, one each for every DOF. The position sensing system is based on a linear potentiometer. The potentiometer wiper is fixed to the cable which varies the voltage proportionately to a change in position, thus providing a reading of the cable movement. The force sensing system is also made up of a linear potentiometer which is connected in parallel to two springs of 6 KN/m each. These springs extend with force application thus giving a change in voltage proportional to the cable tension. Thus, the force sensor makes use of Hooke's Law which states that the extension is proportionate to the load just as long as this load is not too large.

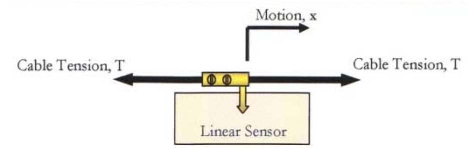

Figure 2: Position Sensor (reproduced from [1])

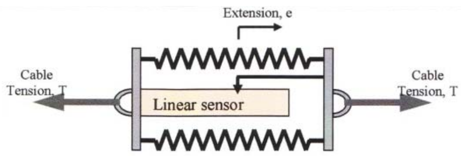

Figure 3: Force Sensor (reproduced from [1])

III MECHANICAL UPGRADING OF THE UOM ROBOT HAND

In this work, upgrading of the robot hand led to the twin actuation system shown in Figure 4. The loop created by the *open* and *close* cables now allows double acting remote actuation. This has added smoothness to the motion of the joints as the opening of the finger joints can also be controlled accurately. Also, no energy is lost in potential energy in the return spring.

A number of other minor improvements were implemented to the basic design of the UOM Robot Hand, some of which are shown in Figure 5. One of these upgrades involved the manufacturing of a threaded hole in each pulley so as to facilitate the fastening of the actuation cables, and thus facilitate dis/assembly. The actuation system was also equipped with new sleeves which secured the positioning of the cable sheaths. This was important so as to increase the robustness of the design. To increase safety, push-to-break switches were also installed for every joint. With such a switch, when the actuation system mechanism of that particular joint reaches its limit, the power to that motor would be restricted to one direction so that the finger joint can only be operated

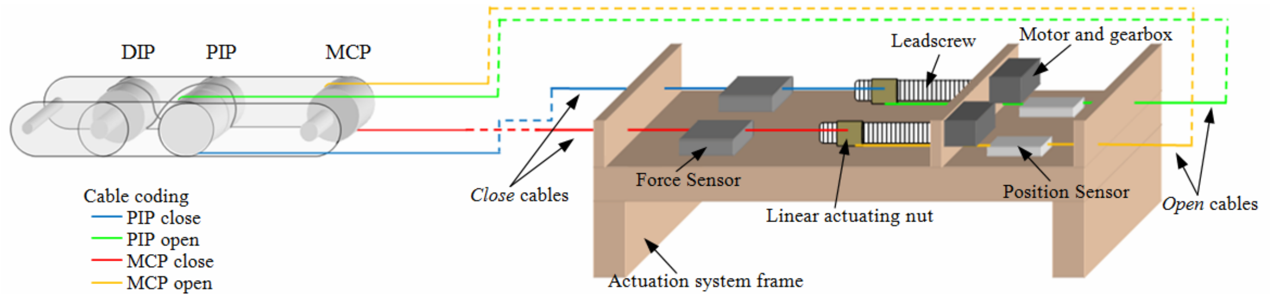

Figure 4: Double-acting actuation and sensing system for one finger

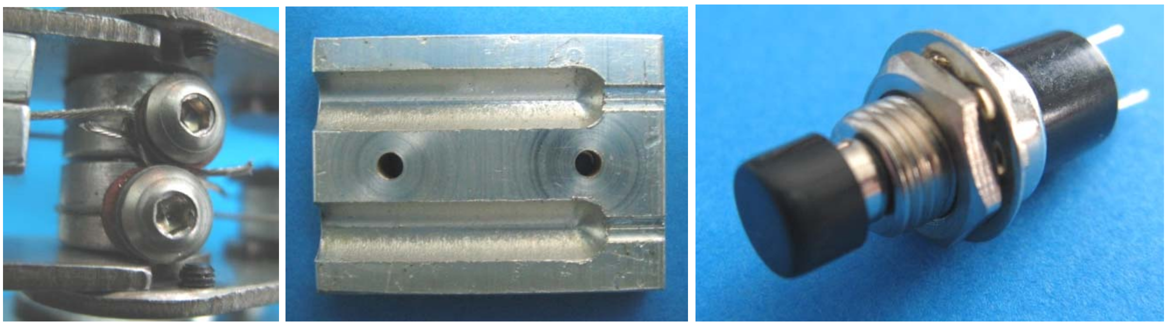

Figure 5: Some of the improvements performed of the basic UOM Robot Hand design: (left to right) Screws fixing cables to the pulleys; New sleeves with manufactured step; Push-to-break switch

away from the limit. Another improvement that took place was the changing of the cable sheaths. The new sheaths installed are made of an extra plastic coating on the inside. This was done in order to decrease the friction between the cable and the sheath. Other minor mechanical improvements were performed so as to increase user friendliness, safety, and stability of the mechanism, and to facilitate further the dis/assembly of the system.

IV COMPUTER INTERFACING

Before calibration of the sensing systems could commence, the potentiometers and their outputs had to be connected to a computer system so that the user could compare multiple results together. The level of interfacing achieved is that of obtaining the voltage readings of all sixteen potentiometers (both position and force sensor readings), translating these readings into angles and fingertip forces respectively, as well as asking the user for the desired angles of each joint and indicating to him/her when the joint is in place.

The hardware used in this system were two NI USB-6009 DAQs with eight analogue input channels each, a Breadboard for easy connections of the various single strand wires involved, a power supply giving a potential difference of 10V at the end terminals of each potentiometer, and a regular computer.

The software needed was designed using Labview Ver. 7.1. Labview uses a graphical programming method. Figure 6(a) shows the necessary icons used, their connections, and their placing to obtain the position sensing results seen in

Figure 66 (b). In these figures, one can see that the voltage value from each channel, which represents a reading from a particular potentiometer, is passed through a formula whose equation was achieved through calibration, and the new values are outputted on counters. These values represent the actual angular position of each joint. The force sensing system used similar software design. However it is meant to involve more formulas as it is split in two stages, that is, the conversion of voltage readings from each potentiometer into tension, and the calculation of the forces at the fingertips, through position and tension readings of the two joints of that particular finger.

The last stage of this program was to allow the users to select the angles which they want the joints to move to. Three LEDs for each joint on the front panel tell the user to open or close the joints, or that the joints are within two degrees of the desired position. This part of the program is shown in Fig. 7.

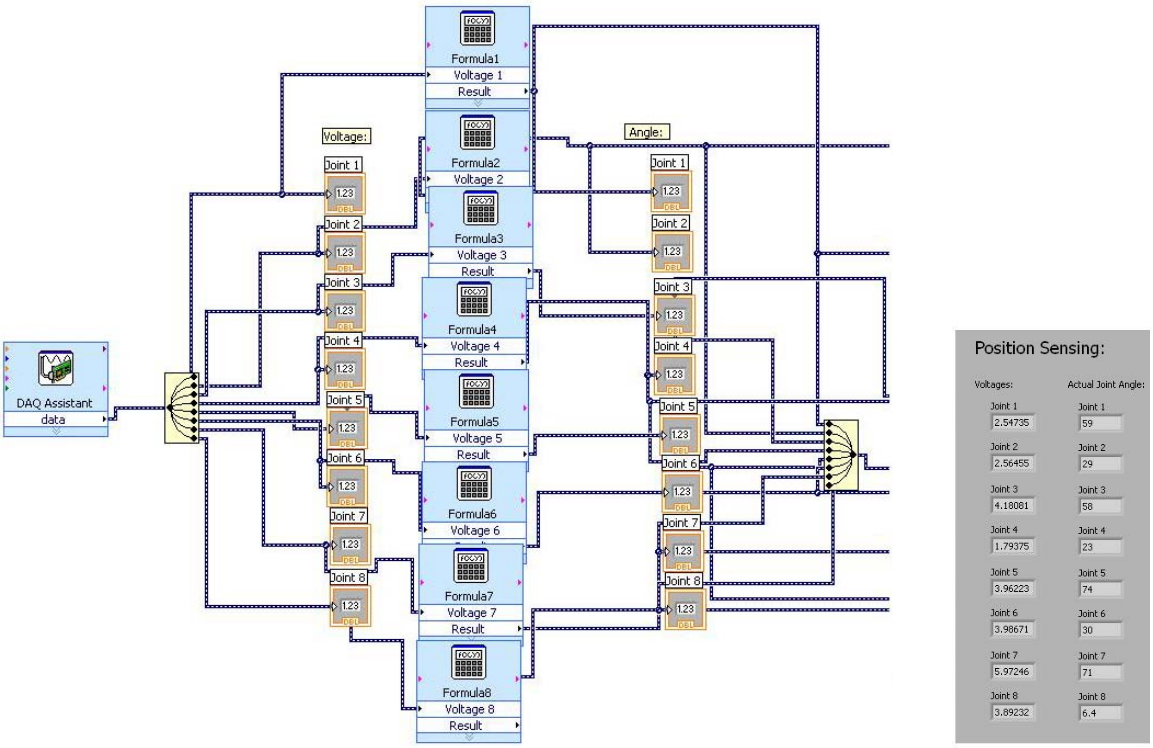

(a) (b)

Figure 6: (a)Block diagram of the position sensing program (b)Front panel display for position sensing

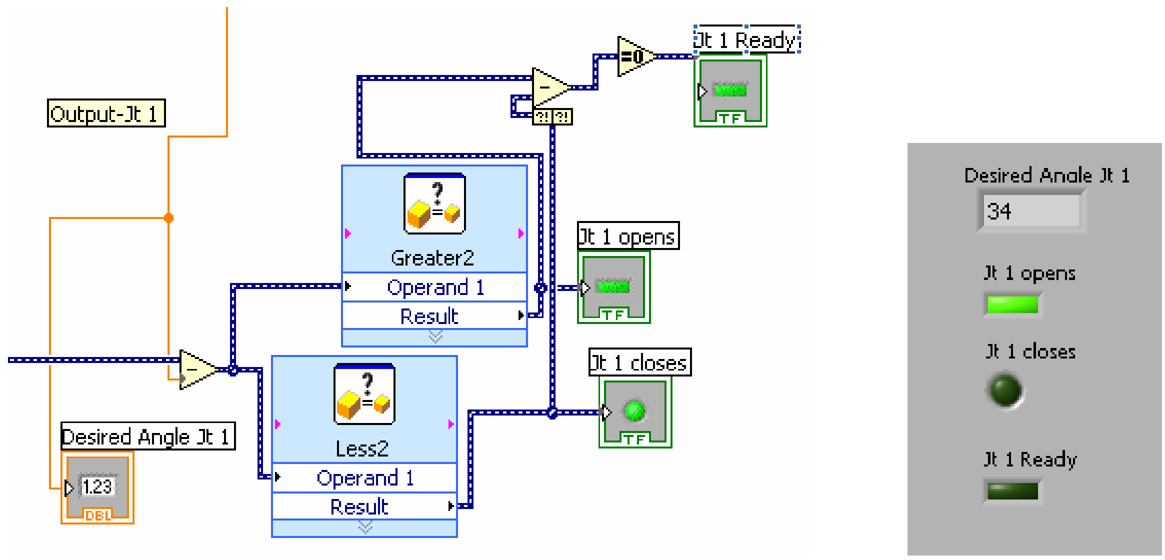

(a) (b)

Figure 7: (a) The block diagram and (b) front panel, for angle selection and indication.

V POSITION SENSING CALIBRATION AND RESULTS

To transform the voltage readings of the position sensors into the respective angles, it was essential to find a relationship for each joint between the voltage reading and the actual angular position of the joint. These relationships were obtained by curve fitting to extensive experimental data, and the equations for all joints were then used in the completion of the computer-based position control system described in Section IV.

A device was custom built for this project so as to allow the angles of both joints to be measured. This device, as attached to the robotic hand, is displayed in Figure 8. One must note that the centre of the larger protractor is aligned with the centre of the joint shaft, whilst the smaller protractor is fastened appropriately to adjust to the angle of the MCP joint. To make this alignment easier, the axis of the shaft centres were joined with a red marker. The reading of the thumb joint angles, as seen in Figure 9, were taken in a slightly different way due to their different structure and functionality.

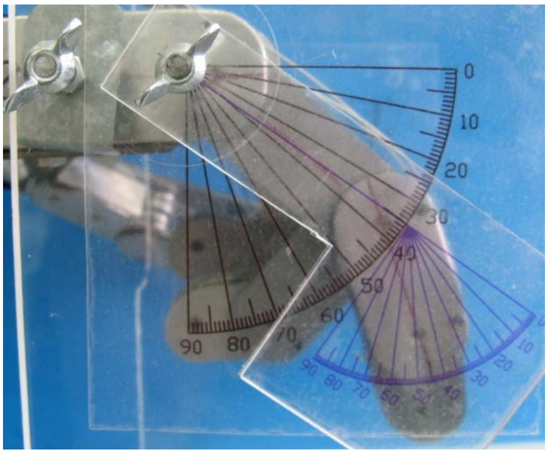

Figure 8: Angle measuring device with the large fixed protractor and the smaller adjustable one

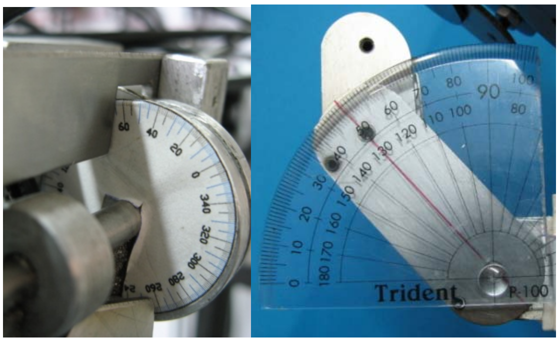

Figure 9: Thumb position calibration

Three sets of readings with fifteen values each were taken for every joint. The readings were then plotted on a number of graphs; one of which is seen in Figure 10. The equation of the curve of best fit for every joint was obtained. The equations for all joints were then inputted in the formulae used by the software created, as described in Section IV above.

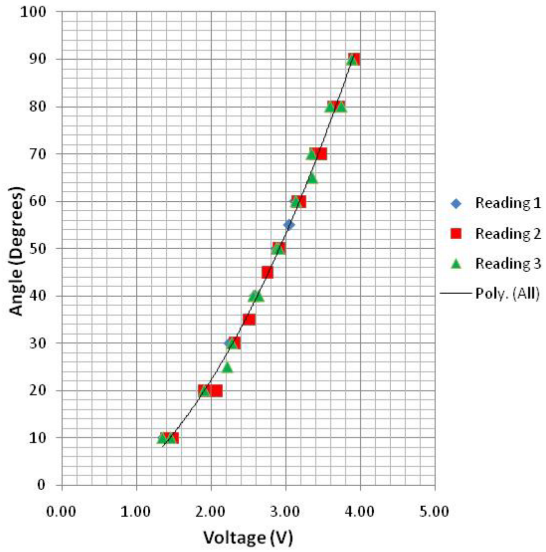

Figure 10: Angle vs. Voltage Graph for the PIP joint of the middle finger

In the next stage an accuracy measurement on each joint was performed. Here, fifteen readings of random positions were taken for each joint, and the true angle was compared to the one displayed by the software, as calculated through the equations obtained by calibration. A summary of the results of these experiments can be seen in Table 1 below.

Joint	Average Error	Maximum Error
Thumb Rotation	0.93°	2°
Thumb Flexion	0.6°	2°
MCP Index	3.13°	6°
PIP Index	1.4°	3°
MCP Middle	2.4°	4°
PIP Middle	3°	5°
MCP Ring	1.73°	4°
PIP Ring	1.6°	5°

Table 1: Results of Accuracy Experiments for all the joints

As can be seen, the results achieved are quite satisfactory. A global average error of only 1.85° and an average maximum error of 3.875° were obtained. One can also see that the thumb flexion joint has an average error of just 0.6° and a maximum error of 2°. These results indicate that remote position sensing can be, in fact, performed with the method used.

It is also believed that better results can be attained if potentiometers of higher quality are used. This is because the variability from one potentiometer to another was high, which resulted in very different relationships between the angles and the voltages of different joints. This limited the comparison of different joints and their results. An even greater source of error both during calibration and during accuracy measurement is parallax error. The chance of a greater error rises as the distance between the angle measuring device and the particular joint being calibrated increases. The prevention of this error proved most difficult in measurements performed on the middle finger since this is furthest from either side of the device, and the view of which is sometimes obstructed by the presence of the other fingers.

VI FORCE SENSING CALIBRATION AND RESULTS

As briefly explained in Section IV, obtaining the fingertip forces for every finger is more complex than position sensing. Force sensing can be split into two main stages. The first stage involves the conversion of the voltage output of the force sensors into a value of the tension experienced by the cable of the particular joint. To obtain this, every sensor was calibrated by loading it with a maximum mass of 44lb (~20kg) whilst taking a reading at every 2lb (~0.91kg). Five such cycles for each sensor were performed, some of which involved the unloading of weights rather than the loading so as to check for hysteresis. The positive outcome of this stage can be seen in Figure 11, where one can notice that all the points on the graph lay in great proximity to the curve of best fit. Certain force sensors, however, showed some constant discrepancy between the loading and unloading readings, as well as some "dead zones" where a change in the mass was not followed by a voltage change. "Dead zones" mostly occurred with a change in the loading sequence (that is, from loading to unloading or vice versa) and at very low masses. The latter case can be clearly seen in Figure 11, where the first 20N increase resulted in practically no change in voltage readings. To reduce this error, one of the two 6KN/m springs was removed. This made the force sensor much more sensitive, reducing the "dead zones" to insignificant errors. Unfortunately with this change, the force sensor lost some of its balance. Thus, the remaining 6KN/m spring should be replaced by two 3KN/m springs for future studies. Another minor modification to increase the accuracy of the force sensors was the use of the potentiometers in a reducing manner. In other words, when the sensor is loaded, the potentiometer output decreases from 10V, rather than increases from 0V. Although this resulted in a graph in which the line of best fit has a negative gradient, the effects of noise on the voltage output is relatively reduced since it is only a very small percentage of a relatively high output voltage.

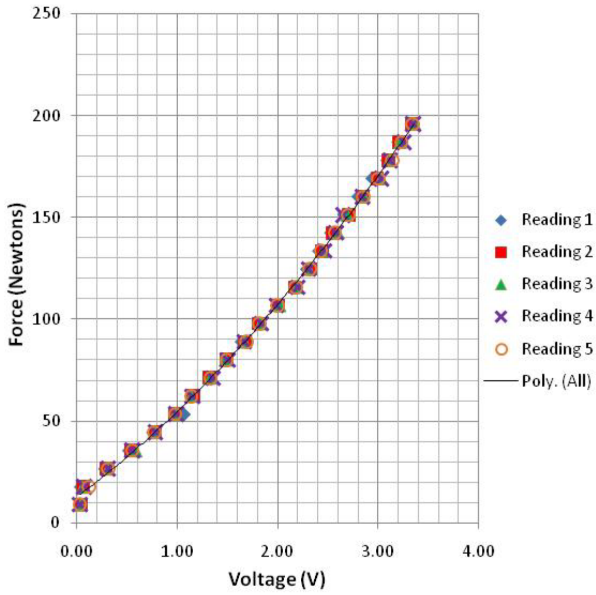

Figure 11: Tension vs. Voltage Graph for the PIP joint of the middle finger

Fingertip force testing was then commenced. For this calibration, a piezoelectric force sensor with a maximum working load of 15N was mounted on a reconfigurable stand which allowed the sensing of the fingertip force in most joint positions. For the preliminary tests, a number of data were gathered with only one variable at a time. An example of this is the graph in Figure 12. Here, Series 1 shows the relationship between the fingertip force and the tension of the MCP joint, with the tension of the PIP joint cable at a constant 5.2N and the angles of the MCP and PIP joints fixed at 28° and 14° respectively. Series 2 shows this same relationship with the tension of the PIP joint cable at a constant 35N and the angles of the MCP and PIP joints fixed at 21° and 39° respectively. These two series show the consistency in the results obtained.

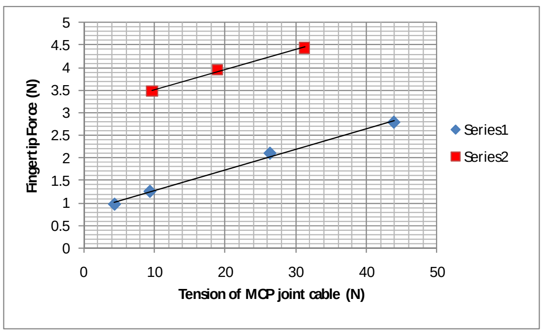

Figure 12: Relationship between Fingertip Force and Tension of MCP joint of ring finger

The results of similar tests on the PIP joint are illustrated in Figure 13, where one can see that the relationship of this joint to the fingertip force is less consistent than that of the MCP joint. Nonetheless, the results obtained are acceptable, since although the gradients of the two series are not exactly the same, minor differences in the parameters are present. Some of the inconsistency is due to the difficulties experienced when increasing the tension of the PIP joint cable since this sometimes altered the joint angle. This resulted in some inaccuracies such as the non-perpendicular contact with the force sensor, as well as the predictable change in force at different angles through kinematic effects.

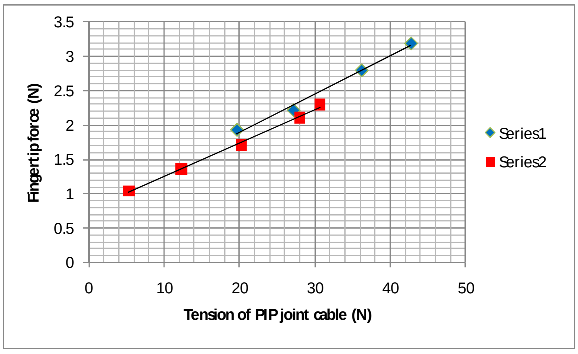

Figure 13: Relationship between Fingertip Force and Tension of PIP joint of ring finger

The last step in the force sensing calibration will involve the calculation of the fingertip force through a formula which links the relationships between all the variables. One such formula is that derived in [1]. However, the calculated force through this formula did not match the actual force obtained from the force sensor readings in our experiment. Unfortunately this theoretical formula neglects the weights of the finger links, and more importantly it neglects the effects of friction. During the course of this project, the reduction of friction was given a lot of importance. One of the major efforts performed was the changing of old cable sheaths to ones which are coated with plastic on the inside. However, although decreased, the effect of friction has so far remained significant.

Another source of error encountered in this hand project, most especially during force sensing experiments, but also to a smaller scale in the position sensing experiment, is the loss of cable tightness. A number of authors on remotely actuated robotic hands with cable transmission complain of this effect. Some of these authors explain their efforts in the attempt at reducing this occurrence [12], [13], [14].

VII Conclusion

In this work, we have built on the results of [1], to gather the lessons taught to us by human anatomy, and we have constructed an anthropomorphic robot hand with remotely located actuation and sensory systems. In this respect, the robot hand mimics the human hand, which has many of its actuators (muscles) and even sensors located in the forearm [2]. In spite of an advanced sensory system, the human hand greatly relies on the very high quality visual feedback produced by the human eyes as well as the sophisticated knowledge base of the human brain. Although cable transmission systems are associated with some inaccuracies [15], these allow adequate precision particularly in cases where the hand is to be used in teleoperations mode, analogous to the method of use of human hands. In such situations, the demands on actuator and sensor accuracy are reduced. Even though some precision is lost due to the distance from the fingers of the robotic hand to the point of sensing, with this work it is shown that the level of accuracy experienced in remote sensing is still acceptable when compared to other sensing methods. The concept of sensing the force and position of the fingers remotely through the cable tension and position has thus been demonstrated.

Remote actuation and sensing can truly be a solution to avoid bulky and cumbersome designs for dexterous anthropomorphic hands. This paper has shown all the improvements to the remote actuation and sensing systems used in the UOM Robot Hand, as well as the calibration and verification experiments performed.

References

[1] M. A. Saliba and M. Axiak. Design of a compact, dexterous robot hand with remotely located actuators and sensors. Proceedings of the 15th IEEE Mediterranean Conference on Control and Automation, Athens, June 2007.

[2] R. E. Page. The Structure of the Hand. In The Psychobiology of the Hand, edited by K. J. Connolly. Mac Keith Press, 1998, pp.115.

[3] S. Jacobsen, E. Iversen, D. Knutti, R. Johnson, and K. Biggers. Design of the Utah/Mit Dexterous Hand. Proceedings of the IEEE International Conference on Robotics and Automation, ICRA86, 1986.

[4] C. Melchiorri and G. Vassura. Mechanical and control features of the UB Hand Version II. Proceedings of the IEEE/RSJ International Conferance on Intelligent Robots and Systems, IROS'92,1992.

[5] A. Caffaz and G. Cannata. The Design and Development of the DIST-Hand Dextrous Gripper. Proceedings of the International Conference on Robotic and Automation (ICRA 1998), Leuven, Belgium, May 1998.

[6] L. Biagiotti, F. Lotti, C. Melchiorri, and G. Vassura. Design Aspects for Advanced Robot Hands. IROS02 Tutorial: Towards Intelligent Robotic Manipulation, Lausanne, September, 2002.

[7] C. M. Seguna, and M. A. Saliba. The Mechanical and Control System Design of a Dexterous Robotic Gripper. Proceedings of the International IEEE Conference on Electronics, Circuits, and Systems (ICECS2001), Malta, September 2001.

[8] M. A. Saliba, D. Camilleri, and M. T. Farrugia. Development of an Anthropomorphic Robot Hand and Wrist for Teleoperation Applications. Proceedings of the IEEE International Conference on Information and Automation (ICIA 2005), Colombo, Sri Lanka, December 2005.

[9] N. Mifsud, A. M. Grech, M. A. Saliba, and S. G. Fabri. Development of an Anthropomorphic Robot Finger: Mechanical and Kinematic Aspects. Proceedings of the 37th International Symposium of Robotics (ISR 2006), Munich, Germany, May 2006.

[10]M. A. Saliba, and C. M. Seguna. A Biologically Inspired Sensor for the Prevention of Object Slip during Robotic Grasping and Manipulation. Proceedings of the International Conference on Intelligent Manipulation and Grasping (IMG04), Genova, Italy, July 2004.

[11]M. J. Farrugia and M. A. Saliba. Optimisation of Anthropomorphic Robot Hand Design through Human Manual Dexterity Testing. Proceedings of the 37th International Symposium of Robotics (ISR 2006), Munich, Germany, May 2006.

[12]M. Kaneko, T. Yamashita, and K. Tanie. Basic considerations on transmission characteristics for tendondrive robots. Proceedings of the 5th International Conference on Advanced Robotics. (1991), pp827–832

[13]C. Melchiorri and M. Kaneko. Robot Hands, in Springer Handbook of Robotics, B. Siciliano and O. Khatib, SpringerLink. Berlin: Springer, 2008, pp 345-360.

[14]L.W.Tsai.Tendon-Driven Manipulators, in Robot analysis: The mechanics of serial and parallel manipulators. New York: Wiley, 1999, pp 333-371.

[15]T. Mouri, H. Kawasaki, K. Yoshikawa, J. Takai, and S. Ito. Anthropomorphic Robot Hand: Gifu Hand III. Proceedings of International Conference, ICCAS2002, pp.1288-1293, 2002.